

Study of the $\nu i_{13/2}^{-1}$ band in $^{189}\text{Pt}^*$

HUA Wei(滑伟)^{1,2;1)} ZHOU Xiao-Hong(周小红)^{1,2;2)} ZHANG Yu-Hu(张玉虎)^{1,2)}
 GUO Ying-Xiang(郭应祥)¹⁾ Oshima M.³⁾ Toh Y.³⁾ Koizumi M.³⁾ Osa A.³⁾
 Hatsukawa Y.³⁾ QI Bin(齐斌)⁴⁾ ZHANG Shuang-Quan(张双全)⁴⁾
 MENG Jie(孟杰)⁴⁾ Sugawara M.⁵⁾

1 (Institute of Modern Physics, Chinese Academy of Sciences, Lanzhou 730000, China)

2 (Graduate University of Chinese Academy of Sciences, Beijing 100049, China)

3 (Japan Atomic Energy Agency, Tokai, Ibaraki 319-1195, Japan)

4 (School of Physics, and State-Key Lab. Nucl. Phys. & Tech., Peking University, Beijing 100871, China)

5 (Chiba Institute of Technology, Narashino, Chiba 275-0023, Japan)

Abstract High-spin levels of ^{189}Pt have been studied with the in-beam γ -spectroscopy method via the $^{176}\text{Yb}(^{18}\text{O},5n)$ reaction at the beam energies of 88 and 95 MeV. The previously known $\nu i_{13/2}^{-1}$ band has been confirmed, and its unfavored signature branch extended up to the $31/2^+$ state. Within the framework of the triaxial particle-rotor model, the $\nu i_{13/2}^{-1}$ band is suggested to be associated with the $11/2[615]$ configuration, and to have triaxial deformation.

Key words high-spin state, configuration, particle-rotor model

PACS 23.20.Lv, 21.60.Ev, 27.70.+q

1 Introduction

The neutron-deficient Pt—Hg nuclei with $A \approx 190$ are located in the well known transitional region, which would be rather soft with respect to γ deformation. The charge-radius changes in the even- A Pt nuclei have been observed in the isotope shift measurements^[1], suggesting a prolate to oblate shape transition from light to heavy Pt nuclei. The critical point where the transition happens is at $A \approx 190$. Therefore, the ^{189}Pt nucleus becomes of particular interest for revealing the deformation revolution in the Pt isotope chain. The level structures as well as the shape of ^{189}Pt would be expected to be rather sensitive to the configurations of the valence neutrons. This is the right reason to extend the level scheme of ^{189}Pt via heavy-ion fusion-evaporation reaction, and to analyze the configurations for the bands concerned. Prior to this work, the low-spin states were studied from the decay of ^{189}Au ^[2, 3], and the rotational band

built on the $\nu i_{13/2}^{-1}$ configuration was reported in the literature^[4, 5], and the band head $13/2^+$ state was identified to be an isomer with a half life of 143 μs .

2 Experiments and results

The excited states of ^{189}Pt were populated via the $^{176}\text{Yb}(^{18}\text{O},5n)$ reaction. A 2.1 mg/cm² isotopically enriched ^{176}Yb foil with a 7.0 mg/cm² Pb backing was bombarded with a ^{18}O beam provided by the tandem accelerator at the Japan Atomic Energy Agency (JAEA). The GEMINI^[6] Gamma-ray detector array, consisting of 14 HPGe's with BGO anti-Compton (AC) shields, was used in this experiment. Six of the detectors had an efficiency of 40% and the others had 70% relative to $3'' \times 3''$ NaI. The detectors were calibrated with ^{133}Ba and ^{152}Eu standard sources both before and after the experiment, and the typical energy resolution was about 2.0—2.4 keV at FWHM for the 1332.5 line of ^{60}Co . X- γ - t and γ - γ - t coincidence

Received 19 December 2008

* Supported by National Natural Science Foundation of China (10825522, 10805058, 10775158), West Light Foundation of the Chinese Academy of Sciences (O803080XBB), National Basic Research Program of China (2007CB815001), Project sponsored by SRF for ROCS, SEM (O803090HGJ), and Chinese Academy of Sciences

1) E-mail: huawei@impcas.ac.cn

2) E-mail: zzh@impcas.ac.cn

©2009 Chinese Physical Society and the Institute of High Energy Physics of the Chinese Academy of Sciences and the Institute of Modern Physics of the Chinese Academy of Sciences and IOP Publishing Ltd

measurements were performed at the beam energies of 88 and 95 MeV, at which energies ^{189}Pt had large yields. Here t refers to the relative time difference between any two coincident γ rays detected within 200 ns. A total of 220×10^6 coincidence events were accumulated. After accurate gain matching, the data were sorted into one symmetric matrix for analyzing the coincidence relationships, and one DCO (Directional Correlations of γ rays deexciting the Oriented states), two ADO (Angular Distribution of γ rays deexciting the Oriented states) matrices for obtaining the multipolarity information.

On the basis of the coincidences with the known γ rays, a new level scheme of ^{189}Pt was established. A partial level scheme was presented in Fig. 1.

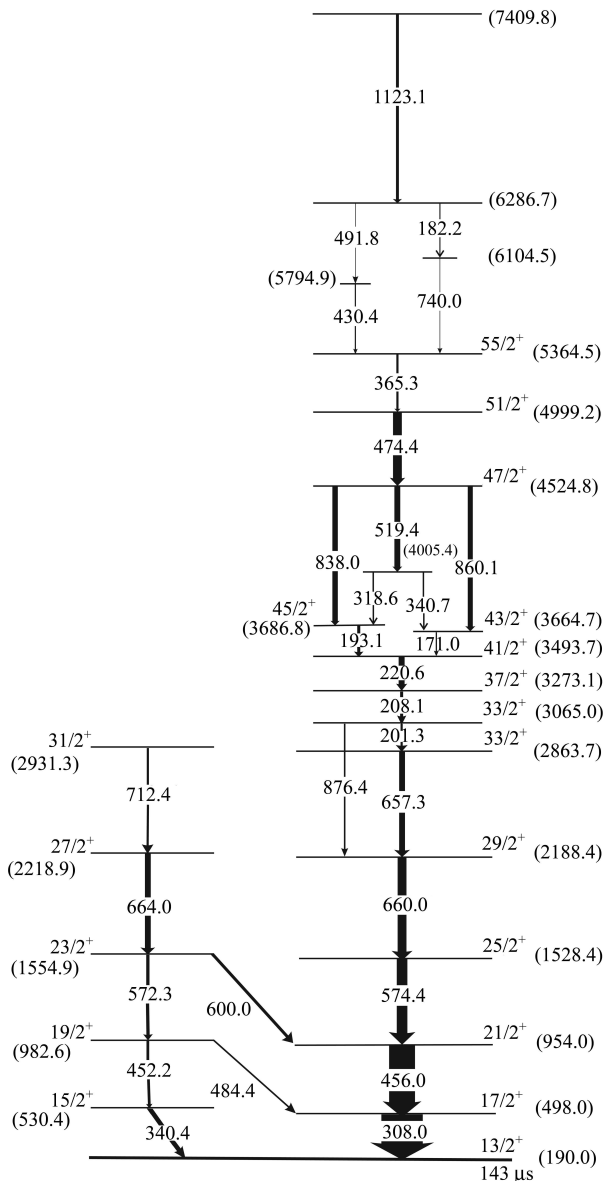


Fig. 1. A partial level scheme in ^{189}Pt deduced from the present work.

A gated spectrum was produced for each of the γ rays assigned to ^{189}Pt . The ordering of the transitions in the scheme was determined according to the γ -ray relative intensities, γ - γ coincidence relationships and γ -ray energy sums. The spins and parities of the levels were deduced from the measured DCO, ADO ratios and the information of the levels previously known. The detailed information was listed in Table 1, including the energies and relative intensities of the γ -ray transitions, spin and parity assignments to the concerned levels and both of the ADO and DCO ratios. In the present experiment, R_{DCO} ratios would be equal to or more than 1.0, and $R_{\text{ADO}} \approx 1.3$ for stretched quadrupole transitions. While for dipole transitions, R_{DCO} would be less than 1.0, and $R_{\text{ADO}} \approx 0.7$. In the new level scheme, the favored signature branch of the $\nu i_{13/2}^{-1}$ band up to the lower $33/2^+$ state was confirmed, and the unfavored one was extended to the $31/2^+$ state. The new structure above the yrast $33/2^+$ state was newly observed in the present work. Two gated spectra are presented in Fig. 2, displaying the coincidence relationship and data quality in the present work.

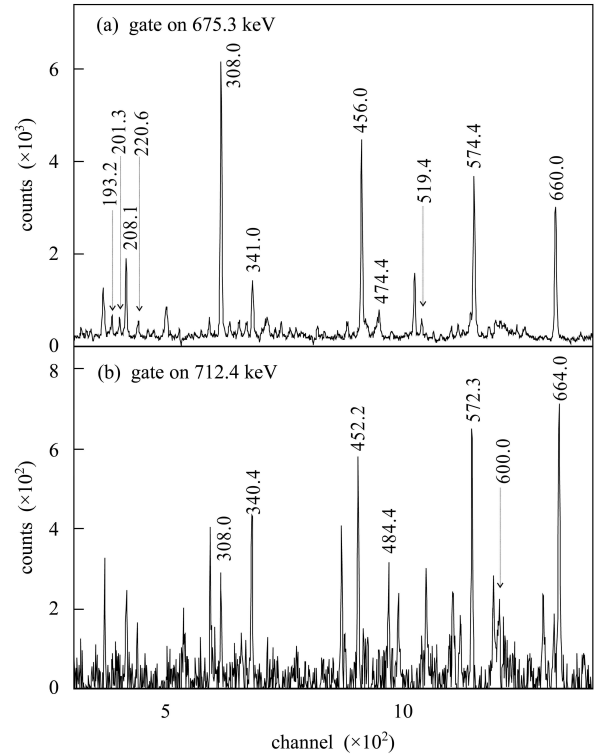


Fig. 2. The γ -ray spectra gated on the (a) 675.3 keV and (b) 712.4 keV transitions.

3 Triaxial particle-rotor model

Various models have been developed to study the nuclei in the transitional region, among which the

Table 1. γ -ray transition energies, initial and final energies of the transitions, spin and parity assignments, relative γ -ray intensities and ADO, DCO ratios in ^{189}Pt .

E_γ/keV	E_i/keV	E_f/keV	$J_i^\pi \rightarrow J_f^\pi$	I_γ^*	R_{ADO}	R_{DCO}
193.1	3686.8	3493.7	$\frac{45}{2}^+ \rightarrow \frac{41}{2}^+$	7.3 ± 0.2	1.23 ± 0.07	$1.25 \pm 0.08^{\text{a}}$
201.3	3065.0	2863.7	$\frac{33}{2}^+ \rightarrow \frac{33}{2}^+$	5.2 ± 3.3	1.23 ± 0.06	$1.48 \pm 0.17^{\text{a}}$
208.1	3273.1	3065.0	$\frac{37}{2}^+ \rightarrow \frac{33}{2}^+$	7.3 ± 0.1	1.28 ± 0.03	$1.21 \pm 0.05^{\text{a}}$
220.6	3493.7	3273.1	$\frac{41}{2}^+ \rightarrow \frac{37}{2}^+$	14.4 ± 0.3	1.21 ± 0.06	$1.15 \pm 0.03^{\text{a}}$
308.0	498.0	190.0	$\frac{17}{2}^+ \rightarrow \frac{13}{2}^+$	100 ± 4.1	1.27 ± 0.04	
365.3	5364.5	4999.2	$\frac{55}{2}^+ \rightarrow \frac{51}{2}^+$	5.2 ± 0.2	1.23 ± 0.07	
430.4	5794.9	5364.5	$\rightarrow \frac{53}{2}^+$	2.7 ± 0.1		
452.2	982.6	530.4	$\frac{19}{2}^+ \rightarrow \frac{15}{2}^+$	6.7 ± 0.2	1.14 ± 0.06	
456.0	954.0	498.0	$\frac{21}{2}^+ \rightarrow \frac{17}{2}^+$	62.6 ± 1.5	1.23 ± 0.03	$1.10 \pm 0.07^{\text{b}}$
474.4	4999.2	4524.8	$\frac{51}{2}^+ \rightarrow \frac{47}{2}^+$	21.3 ± 0.7	1.28 ± 0.05	$1.36 \pm 0.10^{\text{a}}$
484.4	982.6	498.0	$\frac{19}{2}^+ \rightarrow \frac{17}{2}^+$	3.8 ± 0.2	0.34 ± 0.05	$0.34 \pm 0.04^{\text{b}}$
519.4	4524.8	4005.4	$\frac{47}{2}^+ \rightarrow \frac{45}{2}^+$	14.2 ± 0.7	1.24 ± 0.05	$1.02 \pm 0.07^{\text{a}}$
572.3	1554.9	982.6	$\frac{23}{2}^+ \rightarrow \frac{19}{2}^+$	7.8 ± 0.7	1.04 ± 0.07	
574.4	1528.4	954.0	$\frac{25}{2}^+ \rightarrow \frac{21}{2}^+$	25.6 ± 0.9	1.24 ± 0.04	$1.14 \pm 0.10^{\text{b}}$
600.0	1554.9	954.0	$\frac{23}{2}^+ \rightarrow \frac{21}{2}^+$	7.2 ± 0.4	0.52 ± 0.08	
660.0	2188.4	1528.4	$\frac{29}{2}^+ \rightarrow \frac{25}{2}^+$	21.3 ± 0.4	1.15 ± 0.05	$1.11 \pm 0.08^{\text{b}}$
664.0	2218.9	1554.9	$\frac{27}{2}^+ \rightarrow \frac{23}{2}^+$	14.1 ± 0.7	1.17 ± 0.03	
675.3	2863.7	2188.4	$\frac{33}{2}^+ \rightarrow \frac{29}{2}^+$	13.1 ± 0.8	1.35 ± 0.07	$1.09 \pm 0.04^{\text{b}}$
712.4	2931.3	2218.9	$\frac{31}{2}^+ \rightarrow \frac{27}{2}^+$	5.2 ± 0.2	1.42 ± 0.16	
740.0	6104.5	5364.5	$\rightarrow \frac{53}{2}^+$	1.4 ± 0.2		
838.0	4524.8	3686.8	$\frac{47}{2}^+ \rightarrow \frac{45}{2}^+$	13.1 ± 0.4	0.52 ± 0.03	$0.49 \pm 0.04^{\text{a}}$
860.1	4524.8	3664.7	$\frac{47}{2}^+ \rightarrow \frac{43}{2}^+$	15.1 ± 0.7	1.36 ± 0.04	$0.84 \pm 0.08^{\text{a}}$
876.4	3065.0	2188.4	$\frac{33}{2}^+ \rightarrow \frac{29}{2}^+$	3.7 ± 0.2	1.31 ± 0.12	$1.31 \pm 0.08^{\text{a}}$
1123.1	7409.8	6286.7		7.8 ± 0.3		

* Normalized to the 308.0 keV transition. a, b refer to the transitions which the DCO ratios are gating on, and they are E2 type transitions with energies of 660 keV and 308 keV, respectively.

triaxial particle-rotor model (PRM)^[7, 8] is commonly applied to study the configurations of the rotational bands.

The Hamiltonian of an odd- A nucleus can be expressed as

$$\hat{H} = \hat{H}_{\text{rot}} + \hat{H}_{\text{sp}} + \hat{H}_{\text{pair}}, \quad (1)$$

where \hat{H}_{rot} , \hat{H}_{sp} and \hat{H}_{pair} represent the Hamiltonian of the triaxial rotor, the Nilsson type Hamiltonian of the unpaired single particle and the pairing correlation, respectively.

The total wavefunction expanded in the so-called strong coupling basis $|IMK\nu\rangle$ can be written as

$$|IM\rangle = \sum_{K,\nu} C_\nu^{IK} |IMK\nu\rangle. \quad (2)$$

When pairing correlations are neglected, the basis can be expressed as

$$|IMK\nu\rangle = \sqrt{\frac{1}{2}} \sqrt{\frac{2I+1}{8\pi^2}} \times [D_{M,K}^I a_\nu^+ |0\rangle + (-1)^{I-K} D_{M,-K}^I a_\nu^+ |0\rangle],$$

$$K = \dots, -7/2, -3/2, +1/2, +5/2, \dots \quad (3)$$

where $a_\nu^+ |0\rangle$ and $a_\nu^- |0\rangle$ are the single-particle states

which can be written as

$$a_\nu^+ |0\rangle = \sum_{Nlj\Omega} c_{Nlj\Omega}^{(\nu)} \psi_{j\Omega}^{Nl},$$

$$a_\nu^- |0\rangle = \sum_{Nlj\Omega} (-1)^{j-\Omega} c_{Nlj\Omega}^{(\nu)} \psi_{j-\Omega}^{Nl}. \quad (4)$$

To include pairing effects in the PRM, one should replace the single-particle state $a_\nu^+ |0\rangle$ in the basis states (see Eq. (3)) with the Bardeen Cooper Schrieffer (BCS) quasiparticle state $a_\nu^+ |\tilde{0}\rangle$ to obtain a new expansion basis.

4 Discussion

The neutron Fermi level λ_n of ^{189}Pt lies at the top of the $i_{13/2}$ sub-shell, and a decoupled band associated with the $\nu i_{13/2}^{-1}$ configuration was observed systematically in the vicinity of odd- A Pt—Hg nuclei. The structure below the higher $33/2^+$ state shown in Fig. 1 was suggested to be associated with the $\nu i_{13/2}^{-1}$ configuration since it obviously followed the systematic. In the PRM calculation, we take 9 single-particle orbitals near the Fermi surface which are considered to be sufficient to reproduce the experimental data.

The quadrupole deformation parameter β_2 is fixed to be 0.15 due to similar deformation deduced from the neighboring nuclei^[1, 9–11]. Considering the γ -soft character of ^{189}Pt , we carry out a series of calculations by varying γ values to fit the experimental results. It is found that the calculation reproduces the experimental energy spectra and signature splitting pretty well when the triaxiality $\gamma = -30^\circ$. The calculated energy spectra are presented in Fig. 3. The signature splitting is defined as

$$S(I) = \frac{E(I) - E(I-1)}{2I}.$$

The calculated $S(I)$ in comparison with the experimental data is exhibited in Fig. 4, when γ is taken with 0° , -30° and -60° , respectively.

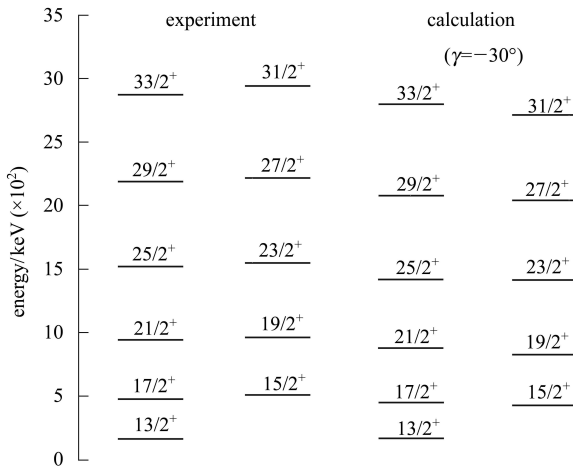


Fig. 3. The energy spectra for the $\nu i_{13/2}^{-1}$ band calculated by the PRM in comparison with the experimental data.

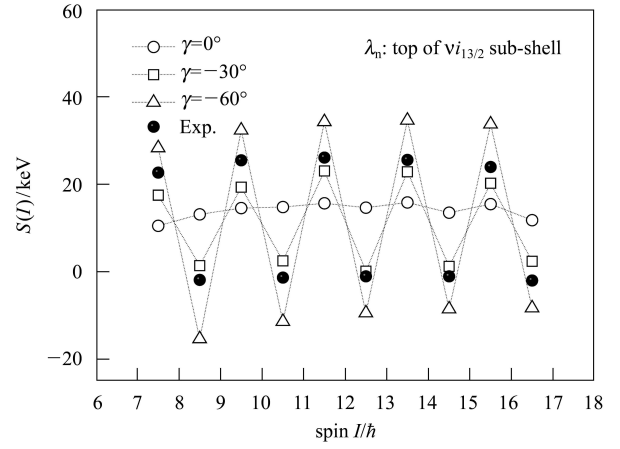


Fig. 4. The signature splitting $S(I)$ for the $\nu i_{13/2}^{-1}$ band calculated by the PRM in comparison with the experimental data.

By diagonalizing the single-particle Hamiltonian, we could obtain the main components of the single-particle orbitals near the Fermi surface in terms of Nilsson levels, as shown in Table 2. The total wavefunction in terms of the single-particle states are listed in Table 3.

From Table 3, we could be convinced of the strong mixing among the single-particle states in the total wavefunctions, when $\gamma = -30^\circ$. The $\nu i_{13/2}^{-1}$ band comes mainly from the 28th neutron-hole single-particle orbital coupling with the triaxial ^{189}Pt core. As listed in Table 2, the 28th orbital contains 93% $|6i_{13/2}11/2\rangle$ configuration. Therefore, the $\nu i_{13/2}^{-1}$ band could be suggested to arise mainly from the $11/2[615]$ configuration.

Table 2. The main components of the single-particle orbitals near the Fermi surface expanded in the basis $|Nlj\Omega\rangle$, when γ takes the value of -30° , 0° and -60° , respectively. ν refers to the index assigned according to the sequence of the energy.

γ	$ \nu\rangle$	wavefunction in terms of $ Nlj\Omega\rangle$
-30°	$ 25\rangle$	$-0.665 6i_{13/2}5/2\rangle - 0.504 6i_{13/2}1/2\rangle + 0.333 6i_{13/2}7/2\rangle$
	$ 26\rangle$	$-0.822 6i_{13/2}7/2\rangle - 0.193 6i_{13/2}1/2\rangle + 0.174 6i_{13/2}11/2\rangle$
	$ 27\rangle$	$-0.929 6i_{13/2}9/2\rangle - 0.159 6g_{9/2}5/2\rangle$
	$ 28\rangle$	$-0.966 6i_{13/2}11/2\rangle - 0.158 6i_{13/2}7/2\rangle + 0.152 6g_{9/2}7/2\rangle$
	$ 29\rangle$	$0.977 6i_{13/2}13/2\rangle + 0.154 6g_{9/2}9/2\rangle$
0°	$ 27\rangle$	$0.986 5i_{13/2}9/2\rangle$
	$ 28\rangle$	$0.995 6i_{13/2}11/2\rangle$
	$ 29\rangle$	$0.997 6i_{13/2}13/2\rangle$
-60°	$ 27\rangle$	$-0.957 6i_{13/2}5/2\rangle$
	$ 28\rangle$	$0.949 6i_{13/2}3/2\rangle$
	$ 29\rangle$	$0.945 6i_{13/2}1/2\rangle$

Table 3. The main components expanded in the strong coupling basis $|IMK\nu\rangle$ (denoted as $|\nu K\rangle$ for short) for selected states, when γ is taken with -30° , 0° and -60° , respectively.

γ	I^π	wavefunction in terms of $ \nu K\rangle$
-30°	$13/2^+$	$-0.565 28\frac{11}{2}\rangle + 0.483 27\frac{9}{2}\rangle - 0.401 29\frac{13}{2}\rangle$
	$15/2^+$	$-0.566 28\frac{11}{2}\rangle + 0.467 27\frac{9}{2}\rangle - 0.401 29\frac{13}{2}\rangle$
0°	$13/2^+$	$-0.738 28\frac{11}{2}\rangle - 0.455 29\frac{13}{2}\rangle - 0.448 27\frac{9}{2}\rangle$
-60°	$13/2^+$	$-0.609 29\frac{1}{2}\rangle - 0.559 28\frac{3}{2}\rangle + 0.452 27\frac{5}{2}\rangle$

From the configuration of the $13/2^+$ state deduced shown in Table 2 and Table 3, we can understand the different trends of the $S(I)$ curves plotted in Fig. 4. When this structure was prolately deformed ($\gamma = 0^\circ$), the valence neutron hole would mainly occupy the $11/2[615]$ Nilsson orbital and there would be no signature splitting. If it had oblate deformation ($\gamma = -60^\circ$), the $1/2[660]$ Nilsson orbital would be mainly occupied by the odd neutron and a large signature splitting could be observed due to the strong Coriolis effect. The calculated signature

splitting fits the experimental data globally well only when a triaxial core ($\gamma = -30^\circ$) is supposed. As discussed above, the $\nu i_{13/2}^{-1}$ band could be considered as a triaxially deformed band ($\gamma = -30^\circ$), and be built mainly on the $11/2[615]$ single-particle configuration. The higher levels are suggested to be associated with multi-quasiparticle configurations which are beyond the PRM method at present.

5 Summary and concluding remarks

The transitional nucleus ^{189}Pt has been produced via the $^{176}\text{Yb}(^{18}\text{O}, 5n)$ reaction. The level scheme has been extended greatly to high-spin states, and the $\nu i_{13/2}^{-1}$ band previously known has been confirmed and revised. By applying the triaxial particle-rotor model, the nature of the $\nu i_{13/2}^{-1}$ band in ^{189}Pt , as well as its deformation information, has been obtained. It is suggested that the $\nu i_{13/2}^{-1}$ band of the transitional nucleus ^{189}Pt might have a triaxial deformation $\gamma = -30^\circ$ and be based on the $11/2[615]$ configuration.

References

- 1 Lee J K P, Savard G, Crawford J E et al. Phys. Rev. C, 1988, **38**: 2985
- 2 Johansson A, Svahn B, Nyman B et al. Z. Phys., 1970, **230**: 291
- 3 Jastrzebski J, Kilcher P, Paris P. J. Phys (Paris)., 1973, **34**: 755
- 4 Piiparinen M, Cunnane J C, Daly P J et al. Phys. Rev. Lett., 1975, **34**: 1110
- 5 WU S C, NIU H. Nuclear Data Sheet, 2003, **100**: 60
- 6 Furuno K, Oshima M, Komatsubara T et al. Nucl. Instrum. Methods A, 1999, **421**: 211
- 7 QI B, ZHANG S Q, WANG S Y et al. HEP & NP, 2006, **30**(Supp II): 112 (in Chinese)
- 8 ZHANG S Q, QI B, WANG S Y et al. Phys. Rev. C, 2007, **75**: 044307
- 9 ZHOU X H, XING Y B, LIU M L et al. Phys. Rev. C, 2007, **75**: 034314
- 10 Kutsarova T, Schück C, Gueorguieva E et al. Eur. Phys. J. A, 2005, **23**: 69
- 11 Ye D, Beard K B, Garg U et al. Nucl. Phys. A, 1992, **539**: 207